Harran Üniversitesi Mühendislik Dergisi

Harran University Journal of Engineering

HU Muh. Der. **01** (2016) p.25-35 HU J. of Eng. **01** (2016) p.25-35

Prediction of Optimal Process Parameters in Hardfacings Obtained by Using Submerged Arc Welding Technique

Mustafa Kaptanoğlu[1], Akın Odabaşı[2], Zafer Aydoğmuş[3]

[1,2] *Department of Metallurgical and Materials Engineering, Faculty of Engineering, University of Firat, Elazig*

[3] *Department of Electrical and Electronic Engineering, Faculty of Technology, University of Firat, Elazig*

e-posta: mkaptanoglu@firat.edu.tr, odabasia@firat.edu.tr, zaydogmus@firat.edu.tr

Received: 03.07.2016 Accepted: 22.08.2016

Abstract

In this study, hardfacings were obtained by using with submerged arc welding powders including different high carbon ferrochromium (4-16 wt.%) and currents from 400 A to 550 A. In order to determine the optimal process parameters in hardfacings, we presented two neural network based predictions with ANN algorithm for chromium and carbon percentages, secondary dendrite arms spacing, cooling rates, macrohardness, and wear loss. The results of ANN performance were presented at two sets of FeCr (wt.%) and net heat inputs in detail. Similarly, two ANN architectures were preferred to obtain the most accurate results. The performance evaluations of the networks were carried out by using Root Mean Squared Error (RMSE), Mean Absolute Error (MAE), and the Coefficient of Correlation, R2, for all models. The models having architecture of 2-15-3 and 2-23-4 were found to be optimal after these criteria. The results showed that the ANNs which helped to decrease number of experimental tests had an acceptable degree of accuracy and great reliability.

Keywords: Submerged arc welding; Hardfacing; High carbon ferrochromium; Prediction; ANN algorithm.

1. Introduction

Submerged arc welding (SAW) is an arc welding method in which an arc creates heat energy required for welding between consumed electrode and work piece. The arc region is occurred between welding powder layer, welding bead, and base metal. Among the welding techniques, submerged arc welding has many advantages such as high melting rate, a mechanised system, a smooth weld metal, very low smoke, high welding rate, low distortion rate, high penetration ability and powder reusability. On the other hand, limited use of electrodes and powders, only suitability for flat and cylindrical parts and applicable only to the thick parts due to the high heat input are disadvantages of the submerged arc welding method [1].

In submerged arc welding, hardfacings are obtained by a combination of powder and wire electrodes. During the submerged arc welding process, alloying elements in powders or alloyed electrodes or both melt to form hardfacing. Alloyed submerged welding powders partially melt and pass in weld metal with unalloyed electrodes and base metal as is in this study. Thus, mechanical properties and chemical composition are improved with alloying elements in hardfacings [2,3].

Because of many parameters and tests, researchers have focused on mathematical modelling by using various methods and computer based programs in order to decrease numbers of repeated experimental tests. Therefore, among the studies including mathematical modelling and prediction of process parameters in submerged arc welding, Kumanan et al., (2007) examined submerged arc welding process with the help of Taguchi technique and regression analysis technique [4]. All factors affecting the welding process were determined by using ANOVA technique as a percentage. As a result of the study, it was stated that the prediction of the welding bead geometry was calculated by using multi-regression technique without any test. In a study conducted by Lu et al., (2014) they investigated to decrease the heat input for the same deposition rate in submerged arc welding process made with two electrodes [5]. For this purpose, they utilised the joint gap. However, they observed that the heat input and current variables also affected the system. Therefore, they stated that the results were achieved to develop with an algorithm including all process parameters. Similarly, Ghosh and Hlock, (2013) aimed to form a mathematical model including welding bead geometry,

mechanical properties, and heat affected zone (HAZ) distance [6]. Accordingly, they utilised the Mat lab, MS Excel computer base programs, and graphical results. Finally, optimal experimental parameters were specified as 50 V (voltage), 600A (current), and 39 cm/ min (travel speed). Nart and Celik, (2013) argued that double ellipsoid models would give more accurate results to determine the weld pool shape [7]. They stated that stress and temperature distributions corresponding to finite element method were predicted by using Abaqus CAE software. As a result of the study, they compared experimental results to evaluate the yield of the double ellipsoid method.

When the other studies in the literature are summarised, researchers generally focus on modelling and prediction of the heat affected zone, [8,9] welding bead height and width, [10,11] temperature distribution [12] and penetration distance [13]. In these studies, mathematical, graphical and software applications were performed and all researchers compared experimental and predicted results. As a result of these comparisons, researchers evaluated suitability of modelling and software programs. Hence, all studies in literature have aimed to decrease a great number of experimental tests, solved the specific problems without any test and predicted to the process parameters.

In this study, unlike the literature, we focused on prediction of the effective parameters on hardfacing. These parameters were obtained with experimental results and these results were modelled with artificial neural network method. Modelled neural network results were compared with experimental results to evaluate the yield of method. Yield of modelling helps to decrease the number of the experimental tests.

2. Experimental

Hardfacings were deposited by using SAW process on SAE 1020 steel in sizes of 10 x 30 x 600 mm. Submerged arc welding machine Magma weld ZD5-1000B, power supply MZ-1000BF, unalloyed S1 welding wire and welding powder having four different high carbon ferrochromium (65 wt.% Cr, 8 wt.% C, Bal. wt.% Fe) powders were used for hardfacings. Table 1 shows chemical compositions of the welding powders.

During the submerged arc welding process, Magma weld power source was used with 400 – 550 A current, 28 V voltage, 50 cm/min travel speed, a 3.2 mm diameter welding wire, direct / constant current mode, and electrode positive polarity. The high carbon ferrochromium content of the powder mixtures varied from 4 wt.% to 16 wt.%. First four samples which have 4wt.% - 16 wt.% high carbon ferrochromium in powders with 500 A currents and last four samples which have 400 A - 550 A with 16 wt.% high carbon ferrochromium in powders employed depending on the welding condition. Other welding process parameters such as voltage, wire diameter, and travel speed were kept constant during all the experiments.

Samples in the size of 1 x 1 x 1 cm taken from the cross-section of the hardfacings were prepared by using metallographic method. EDS composition analysis was performed with Jeol (JXA-8230, USA) and secondary dendrite arms spacing was measured by using Nikon (Eclipse-MA200, Japan) optical microscopy on the seam surface and cross-section view of the samples. Secondary dendrite arms spacing was determined based on mean values of results taken from 30 different zones of each sample. Figure 1. shows the measurement of secondary dendrite arms spacing as a representative image.

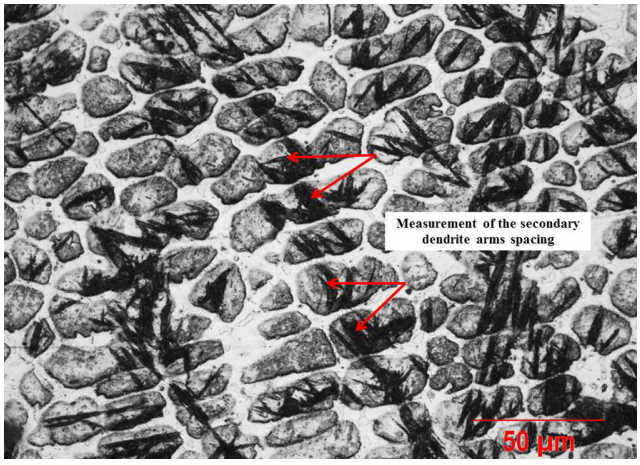

Figure 1. Measurements of the secondary dendrite arms spacing for hardfacing made by sample ID 2 at 500 A.

Table 1. Chemical composition for the submerged arc welding powders.

	Chemical composition (wt.%)								
Powder ID	FeCr	CaO	TiO_2	MnO	(Na_2O +K_2O)	CaF_2	FeMn	FeMo	Elazig ferrochromium slag
1	4	3-7	4-8	3-7	1-2	5-15	1-3	0.5-1.5	56.5-65.5
2	8	3-7	4-8	3-7	1-2	5-15	1-3	0.5-1.5	52.5-61.5
3	12	3-7	4-8	3-7	1-2	5-15	1-3	0.5-1.5	48.5-57.5
4	16	3-7	4-8	3-7	1-2	5-15	1-3	0.5-1.5	44.5-53.5

As is well-known; the heat input is directly related with dendrite arms spacing and cooling rate. Therefore, heat input and its effect on weld region must be well known. Hence, heat input which was occured during the submerged arc welding process and arc energy efficiency should be calculated. Calculation of the heat input [14,15];

$$H=60.E.I / 1000\ S \quad (1)$$

where H is heat input or arc energy (kj/inch or kj/mm), E is arc voltage, I is current and S is travel speed (inch/min or mm/min).

Net heat input may be obtained by multiplying with effect factor or efficiency coefficient in Table 2. It is seen that submerged arc welding process efficiency factor is 1. Thus, submerged arc welding was carried out with maximum efficiency [16,17].

$$HI=\eta.\ H \quad (2)$$

where HI is net heat input (kj/inch or kj/mm) and η is efficiency factor coefficient.

Recently, heat input calculation formula is derived from more than two above-mentioned formulas. Kou, (2003) reported that these formulas were different from traditional formulas by means of using parameters such as weld beam length and arc time in heat input [17]. However, net heat input was calculated by using traditional heat input formula in this study and arc voltage and welding speed were kept constant for all samples. For this reason; the most important variable was current or heat input in formula was observed.

Table 2. Efficiency factor coefficients for different welding processes [18].

Process	**Efficiency factor coefficient**
Submerged arc welding (SAW)	1.0
Manuel metal arc (MMA)	0.8
Cored wire welding / flux cored arc welding(FCAW)	0.8
Metal active gas/metal inert gas(MIG/MAG) Gas metal arc welding (GMAW)	0.8
Tungsten inert gas (TIG)/ Gas tungsten arc welding (GTAW)	0.6
Plasma arc welding	0.6

The cooling rate depending on the secondary dendrite arms spacing was calculated by the following formulas in references respectively [18-21].

Formula 1; $\lambda = 104.47 \times T^{-0.310}$ (3)

Formula 2; $\lambda = 156.52 \times T^{-0.349}$ (4)

Formula 3; $\lambda = 148 \times T^{-0.38}$ (5)

Formula 4; $\lambda = 68 \times T^{-0.45}$ (6)

Where λ is secondary dendrite arms spacing (µm) and T is cooling rate (ºC/Sec).

Among these formulas, formula 1 and 2 are preferred to calculate the cooling rate for nickel based materials. The formula 3 is preferred when the steel contains C of 0-0.53 wt.%. Formula 4 is preferred to calculate cooling rate of ASTM 304 stainless steel. In this study, Formula 4 was chosen to calculate the cooling rate due to the similarity with ASTM 304 stainless steel and possible composition of the hardfacing.

Macrohardness tests were carried out by using HRC (Rockwell-C) scale under a 150 kgf (1471.5 N) load. Macrohardness was measured from the cross section of the hardfacings as an average values which was taken 10 different locations. Wear tests were carried out by using pin-on-disc method and 30 N load, 20 m sliding distance and 80 mesh abrasive paper were employed to determine the wear loss of harfacings and wear losses were calculated as a percentage for more objective results.

3. Experimental results and determination of input and output parameters

Table 3 shows experimental results of the hardfacing. When the experimental results were analysed depending on increasing percentage of the ferrochromium in powder (4-16 wt.%) at 500A (Sample ID 1-4), net heat input was found to be constant because of the constant current. According to the EDS analysis results, chromium and carbon percentages increased from 3.12 wt.% to 7.13 wt.% and 1.65 wt.% to % 2.12 wt.% respectively. With the increasing amount of ferrochromium in powder, chromium and carbon percentage of the hardfacing also increased. When secondary dendrite arms spacing and cooling rates were analysed, dendrite arms spacing was shrunk and cooling rates increased with the increasing percentage of chromium and carbon in hardfacing samples. Accordingly, when macrohardness and wear loss (wt.%) results were analysed, hardness results increased from 34 to 46 HRC and wear losses decreased from 5.01 wt.% to 4.41 wt.%. In this condition, with the increasing amount of the chromium and carbon passing in hardfacing, secondary dendrite arms spacing were shrunk; accordingly, cooling rates, hardness, and wear resistance increased.

When the experimental results were analysed depending on increasing currents of 400-550A for 16 wt.% FeCr (Sample ID 5-8), net heat input increased from 1.08 kj/mm to 1.62 kj/mm. Passed chromium percentage increased from 3.51 wt.% to 7.60 wt.% and carbon also increased from 1.70 wt. % to 2.19 wt.%. With the increasing of net heat input, secondary dendrite arms spacing expanded and cooling rates decreased. When the hardness results were analysed, hardness results increased from 37 HRC to 53 HRC. Unlike the first four samples, expanded secondary dendrite arms spacing and decreasing cooling rates increased hardness results. In this condition, increasing content of the passed chromium and carbon in hardfacings, triggered the martensitic transformation for low cooling rate and transformation delay. Considering hardfacing microstructures; martensite, austenite and carbides phases were stable. Because of the allothropic transformation, heat input and composition of hardfacing were affected the experimental results. Finally, when the wear losses (wt.%) were analysed, wear losses decreased from 4.88 wt.% to 3.90 wt.% because of increased hardness.

At the end of the all experimental results, net heat input and increasing amount of high carbon ferrochromium in powders were affected all experimental results were observed. Therefore, net heat input and increasing amount of ferrochromium in powders were determined as input data, passed chromium and carbon percentage in hardfacings, secondary dendrite arms spacing, cooling rate, hardness, and wear losses (wt.%) were determined

Table 3. Experimental results of hardfacings produced.

Sample ID	Ferrochromium in powder (wt.%)	Current (A)	Net heat input (kj/mm)	EDS analysis (wt.%) Cr	EDS analysis (wt.%) C	Secondary dendrite arms spacing (μm)	Cooling rate Formula 4, (C°/Sec) $\lambda = 68 \times T^{-0,45}$	Hardness (HRC)	Wear loss (wt.%)
1	4	500	1.44	3.12	1,65	19.24 (± 2.12)	1.64x10	34	5.01
2	8	500	1.44	4.03	1.77	17.46 (± 2.51)	2.04x10	39	4.76
3	12	500	1.44	6.55	1.99	16.11 (± 3.01)	2.44x10	43	4.50
4	16	500	1.44	7.13	2.12	15.08 (± 3.57)	2.81x10	46	4.41
5	16	400	1.08	3.51	1.70	13.12 (± 2.75)	3.85x10	37	4.88
6	16	450	1.26	5.40	1.88	14.39 (± 2.43)	3.13x10	41	4.65
7	16	500	1.44	7.13	2.12	15.08(± 3.57)	2.81x10	46	4.41
8	16	550	1.62	7.60	2.19	18.05 (± 2.86)	1.89x10	53	3.90

as output data to predict the optimal process parameters with Matlab programme. In this direction, we prepared two ANN architecture which have the same input and output data due to the first four samples having different ferrochromium percentages in powder and last four samples having different net heat inputs.

4. Prediction of the experimental results

4.1. ANN Algorithm

ANN is a computer-based program that can be used in an effective way in nonlinear systems and other systems. Neural networks are the basic information processing structure consisting of connected neurons. Neural networks are sending signals with weighted connections to communicate with each other. In the training process, learning rule modifies the connection weight. Learning process is a mathematical method that improves the performance of the neural network via biases and the weights determined with the training data set prepared in the training process. Followıng to this process, test data are employed for net validation control. Starting point of weights and biases are determined randomly. In here, activation function is employed for the calculation of the output neurons. Input signals (xi) sums with the each neuron in the hidden layer and these results multiply with the respective connection weights (wji) to determine the output data (yj) that is calculated as a function of the sum;

$$y_j = f\left(\sum w_{ji} x_i\right)$$

In this formula, f is a activation function which is required to convert the sum of signals contacting to the neuron. A sigmoidal activation function is employed for the aim of output neuron calculation. E, is represented with the sum of squared differences between the desired and actual values of the output neurons is given by;

$$E = \frac{1}{2}\sum_j (y_{dj} - y_j)^2$$

Where (ydj) represents the desired output value of neuron, the neuron (j) and (yj) represent the actual output value of neurons [22].

Number of studies preperad with the ANN architecture are available in the literature. Researchers such as Ghosh and Hlock, (2013) and Towsyfyan et al., (2013) compared submerged arc welding experimental results with artificial neural network (ANN) results in their studies [6,23]. At the end of their studies, they stated that more accurate and compatible results were determined with ANN architecture to obtain an experimental design. Therefore, we preferred ANN algorithm in this study as well. In accordance with this purpose, back-propagation learning algorithm was employed in feed forward neural network. Neural network comprise of an input layer, a hidden layer, and an output layer. Schematic image of the multilayer feed-forward network used in this study is given in Figure 2.

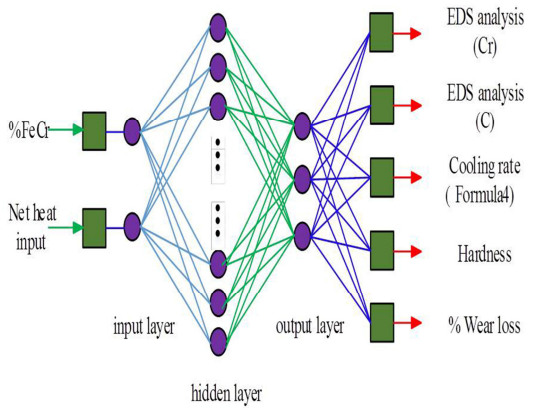

Figure 2. Schematic diagram of proposed ANN.

In the study, two data groups were used for training and testing. While four of eight data were employed for the aim of training in the first step, the other four data were employed for the aim of testing in the second. In order to achieve best architecture of ANN compatible with experimental results, randomly decided three neuron numbers on layers 2-15-3, 2-7-7-3 and 2-23-3 were used to obtain the optimum ANN1 and other three neuron numbers on layers 2-23-4, 2-17-3 and 2-21-3 were used to obtain the optimum ANN2.

Performance evaluation of the network were held on the basis of three criteria. The first, Root Mean Square Error (RMSE), the second, Coefficient of determination (R2) and the third, Mean Absolute Error (MAE) and these are given by;

$$RMSE = \sqrt{\frac{\sum_{i=1}^{n}(y_{pre,i}-y_i)^2}{n}}$$

$$R^2 = 1 - \frac{\sum_{i=1}^{n}(y_{pre,i}-y_i)^2}{\sum_{i=1}^{n}(y_{mea,i})^2}$$

$$MAE = \frac{\sum_{i=1}^{n}|y_{pre,i}-y_i|}{n}$$

Where (n) is the number of data sample, (ypre,I) is the predicted value and (yi) is the value of a data sample.

In order to determine best architecture of ANN compatible with experimental results, great number of neurons in layers were employed. As is seen in all tables, 2-15-3 is more optimal structure for ANN1 compared to others. It had R2 value of 0.9995, RMSE value of 0.0449, and MAE value of 0.1287. For ANN2, the best structure was 2-23-4 and it had R2 value of 0.9996, RMSE value of 0.0438, and MAE value of 0.1343.

Learning algorithm was determined with the help of Levenberg-Marquardt back propagation algorithm, because of giving good performance in both ANNs. When a sigmoidal activation function was employed for the aim of neurons located in input and hidden layers, linear activation function was employed for the aim of neurons located in output layers. While Table 4 shows the evaluation of ANN1, Table 5 shows the measured and predicted values.

Table 4. The performance of ANN1.

Algorithm	R^2	RMSE	MAE
2-15-3	0.9995	0.0449	**0.1287**
2-7-7-3	0.9990	0.0642	**0.2293**
2-23-3	**0.9993**	**0.0547**	**0.1566**

Figures 3-7 show respectively the EDS analysis results for chromium and carbon percentage, secondary dendrite arms spacing, cooling rate, hardness and wear loss (wt.%) versus FeCr (wt.%) and net heat input. As is seen in Table 5, percentage value of FeCr in powders changed from 4 wt.% to 16 wt.%; whereas, net heat input was constant.

Table 5. The measured and predicted values by ANN1.

Ferrochromium in powder (wt.%)		**4**	**8**	**12**	**16**
Net heat input (kj/mm)		1.44	1.44	1.44	1.44
EDS analysis -Cr (wt.%)	Measured	3.12	4.03	6.55	7.13
	Predicted	3.0208	4.1489	6.5175	7.1031
	Error	-0.0992	0.1189	-0.0325	-0.0269
EDS analysis -C (wt.%)	Measured	1.65	1.77	1.99	2.12
	Predicted	1.6423	1.7929	2.0112	2.0826
	Error	-0.0077	0.0229	0.0212	-0.0374
Secondary dendrite	Measured	19,24	17,46	16,11	15,08
arms spacing (µm)	Predicted	19.1230	17.4460	15.9944	15.0157
	Error	-0.1170	-0.0140	-0.1156	-0.0643
Cooling rate	Measured	16.4	20.4	24.4	28.1
Formula 4 (C˚/Sec)	Predicted	16.3396	20.5887	24.3938	27.9880
	Error	-0.0604	0.1887	-0.0062	-0.1120
Hardness (HRC)	Measured	34	39	43	46
	Predicted	34.1705	38.9069	43.0565	46.0644
	Error	0.1705	-0.0931	0.0565	0.0644
Wear loss (wt.%)	Measured	5.01	4.76	4.5	4.41
	Predicted	5.0137	4.7030	4.4945	4.4440
	Error	0.0037	-0.0570	-0.0055	0.0340

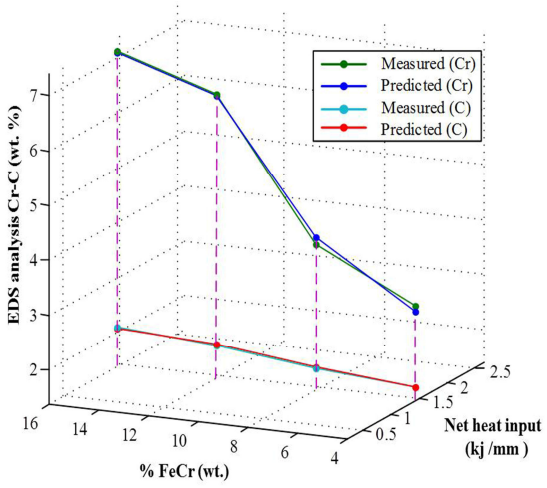

Figure 3. EDS analysis versus FeCr (wt.%) and net heat input.

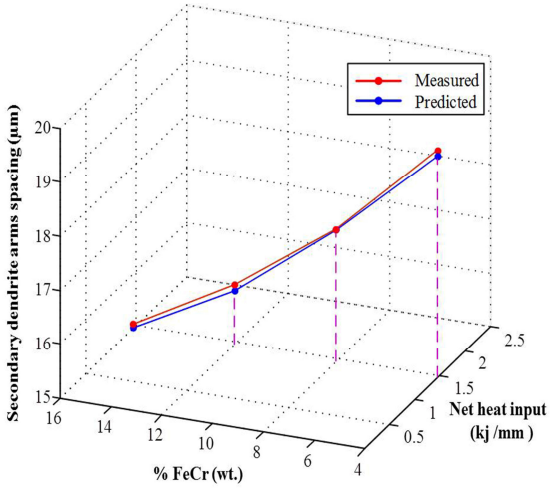

Figure 4. Secondary dendride arms spacing versus FeCr (wt.%)-Net heat input.

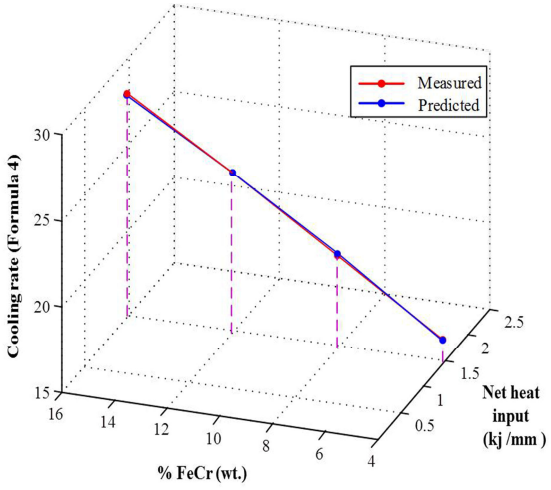

Figure 5. Cooling rate (Formula 4) versus FeCr (wt.%)-Net heat input.

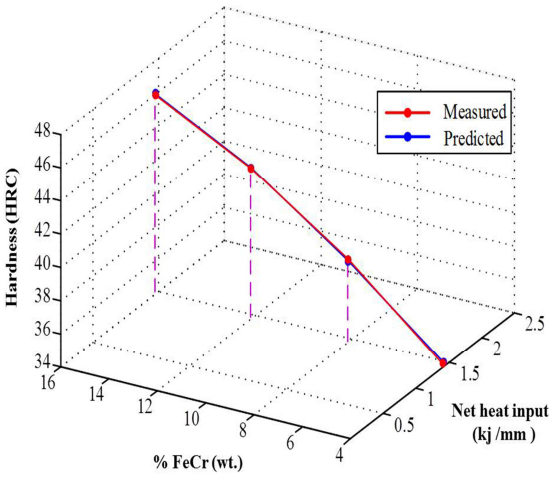

Figure 6. Hardness versus FeCr (wt.%) -Net heat input.

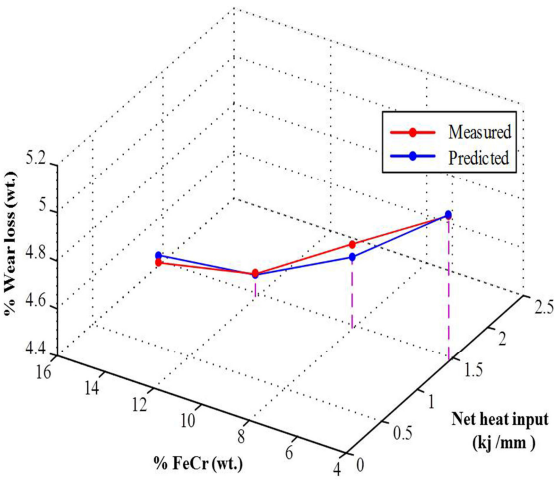

Figure 7. Wear loss (wt.%) versus FeCr (wt.%)-Net heat input.

As is seen in above Figures 3-7 the ANN model had very good estimation ability. The differences between measured and predicted values were very low and acceptable.

The second ANN algorithm was developed to estimate the EDS analysis results for chromium and carbon percentage, secondary dendrite arms spacing, cooling rate, hardness and wear loss (wt.%) with the inputs of FeCr (wt.%) and net heat input. The performances of ANN2 and estimation results are present in Tables 6 and 7, respectively. Graphical results are shown from Figure 8 to 12. As is seen in Table 7, net heat input values changed from 1.08 to 1.62; whereas, FeCr (wt.%) was constant.

Table 6. The performance of ANN2.

Algorithm	R^2	RMSE	MAE
2-23-4	0.9996	0.0438	**0.1343**
2-17-3	0.9961	0.0536	**0.2129**
2-21-3	**0.9994**	**0.0502**	**0.1496**

The graphical results from Figure 8 to 12 show that the ANN2 had a very successful performance in giving the results very close to measured values. Both ANN1 and ANN2 had a very good performance for estimating the results. This helps to reduce the number of experiments and prevents time-consuming procedures.

Table 7. The measured and predicted values by ANN2.

Ferrochromium in powder (wt.%)		**16**	**16**	**16**	**16**
Net heat input (kj/mm)		1.08	1.26	1.44	1.62
EDS analysis - Cr (wt.%)	Measured	3.51	5.4	7.13	7.6
	Predicted	3.4377	5.3488	7.1191	7.6064
	Error	-0.0723	-0.0512	-0.0109	0.0064
EDS analysis - C (wt.%)	Measured	1.7	1.88	2.12	2.19
	Predicted	1.7017	1.8778	2.0418	2.2226
	Error	0.0017	-0.0022	-0.0782	0.0326
Secondary dendrite	Measured	13.12	14.39	15.08	18.05
arms spacing (µm)	Predicted	13.2153	14.2417	15.1150	17.8854
	Error	0.0953	-0.1483	0.0350	-0.1646
Cooling rate	Measured	38.5	31.3	28.1	18.9
Formula 4 (C˚/Sec)	Predicted	38.2808	31.0369	27.9360	18.9050
	Error	-0.2192	-0.2631	-0.1640	0.0050
Hardness (HRC)	Measured	37	41	46	53
	Predicted	36.9990	41.0734	46.1830	52.9452
	Error	-0.0010	0.0734	0.1830	-0.0548
Wear loss (wt.%)	Measured	4.88	4.65	4.41	3.9
	Predicted	4.8573	4.6520	4.4497	3.8459
	Error	-0.0227	0.0020	0.0397	-0.0541

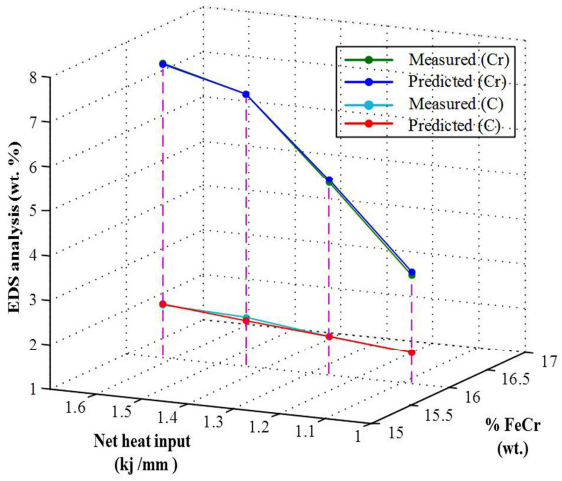

Figure 8. EDS analysis versus FeCr (wt.%)-Net heat input.

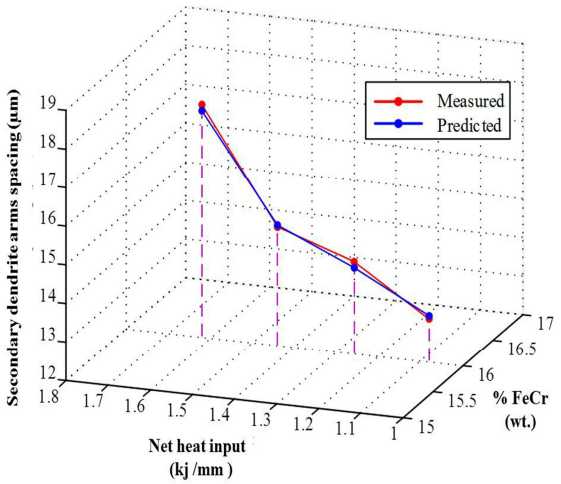

Figure 9. Secondary dendrite arms spacing versus FeCr (wt.%)-Net heat input.

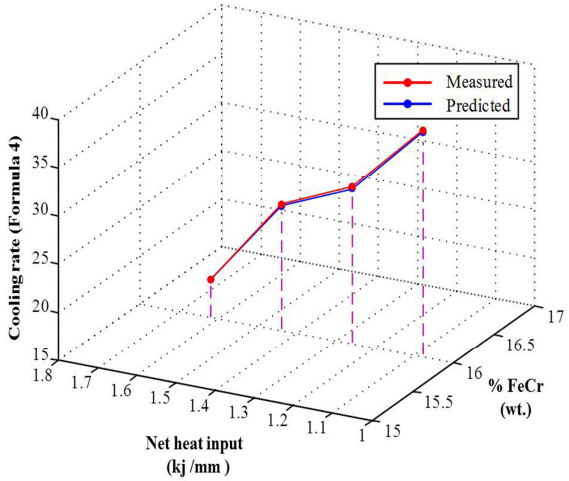

Figure 10. Cooling rate (Formula 4) versus FeCr (wt.%)-Net heat input.

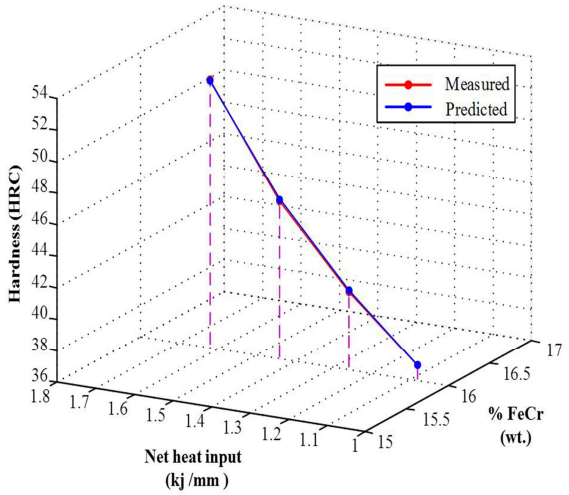

Figure 11. Hardness versus FeCr (wt.%)-Net heat input.

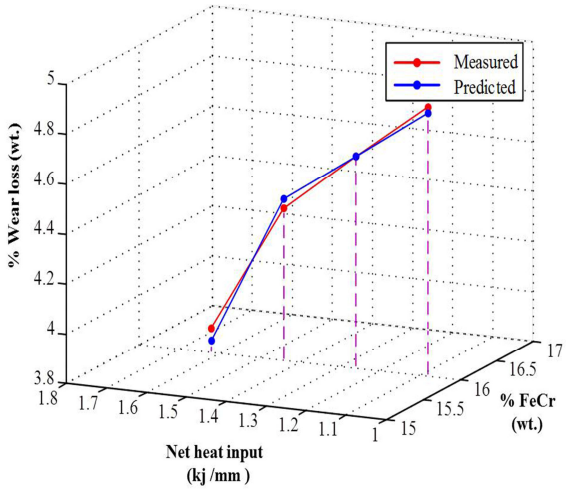

Figure 12. Wear loss (wt.%) versus FeCr (wt.%)-Net heat input.

5. Conclusion

Modelling and predictions could be made by using with the input data such as heat input and welding powder including high carbon ferrochromium, and output data such as EDS chromium and carbon composition, secondary dendrite arms spacing, cooling rate, hardness and wear loss (wt.%) in ANN algorithm were observed. The results obtained from this study can be given as follows,

1.Increasing amount of high carbon ferrochromium in powders and increasing of heat input from 400 A to 550 A, chromium and carbon percentages in hardfacings were increased. Consequently, cooling rate changed and estimating quantity of martensite phases in hardfacings, hardness, and wear resistance increased.

2.ANN algorithm was performed with two different ANN architectures to obtain optimal process parameters. Two different input data were preferred to predict chromium and carbon percentages, secondary dendrite arms spacing, cooling rate, hardness, and wear loss as an output data. First input data was heat input and the second one was increasing quantity of ferrochromium in powders and experimental results and predicted results were compared with these input and output data for optimal ANN algorithm model.

3.2-15-3 and 2-23-4 architectures played a key role to obtain more accurate results by using ANN algorithm and results predicted by ANN algorithm were in good agreement with experimental results.

4. Experimental results of hardfacing performed by using submerged arc welding powders including ferrochromium and device parameters could be modelled and predicted with ANN an algorithm. The design of the experimental results from the hardfacing with alloyed electrode and / or alloyed submerged arc welding powder can be applied with ANN algorithm in the future studies.

Acknowledgement

This study was supported by a grant from the scientific and technological research council of Turkey, TUBITAK (Project No: 114M016). The authors thank the laboratory staff of the

Department of Metallurgical and Materials Engineering in Firat University, (TR) for their efforts to set up the experimental design.

References

[1] J. R. Davis, (ed.), *Welding, Brazing and Soldering*. Volume 6. 10th Editions. Metals Park, ASM International, pp. 699-828, 1993.

[2] J.F. Lancaster, *Metallurgy of Welding*, George Allen Unwin, England, 6th Ed., 1999.

[3] R.Oates, A.M. Saitta, *Welding Handbook, Materials and Applications*, Volume 6, American Welding Society. Miami, FL, 33126., 2000.

[4] S. Kumanan, J. Edwin Raja Dhas, K. Gowthhaman, ''Determination of submerged arc welding process parameters using Taguchi method and regression analysis,'' *Indian Journal of Engineering & Materials Sciences*, Vol. 14, pp. 177-183, 2007.

[5] J. Lu, J.S. Chen, Y.M. Zhang, L. Kvidahl, ''Predictive control based double-electrode submerged arc welding forfilet joints,'' *Journal of Manufacturing Processes*, Volume 16, pp. 415–426, 2014.

[6] A. Ghosh, S. Hloch, ''Predıctıon and optımızatıon of yİeld parameters forsubmerged arc weldıng process,'' *Technical Gazette*, (20-2), pp.213-216, ISSN 1330-3651 (Print), ISSN184-6339, 2013.

[7] E. Nart, Y. Celik, ''A practical approach for simulating submerged arc welding process using FE method,'' *Journal of Constructional Steel Research*, Volume 84, pp. 62–71, 2013.

[8] A. Ghosh, S. Chattopadhyaya, R.K. Das, P.K. Sarkar, ''Assessment of Heat Affected Zone of Submerged Arc Welding Process through Digital Image Processing,'' *Procedia Engineering*, Volume 10, pp. 2782–2785, 2011.

[9] S. Moeinifar, A.H. Kokabi, H.R.M. Hosseini, ''Effect of tandem submerged arc welding process and parameters of Gleeble simulator thermal cycles on properties of the intercritically reheated heat affected zone,'' *Materials and Design*, Volume 32, 869–876, 2011.

[10] S. Karaoglu, A. Secgin, ''Sensitivity analysis of submerged arc welding process parameters,'' *Journal of Materials Processing Technology*, Volume 202, pp. 500–507, 2008.

[11] D.W. Cho, D.V. Kiran, W.H. Song, S.J.Na, ''Molten pool behavior in the tandem submerged arc welding process,'' *Journal of Materials Processing Technology*, Volume 214, pp. 2233–2247, 2014.

[12] V. Negi, S. Chattopadhyaya, ''Critical Assessment of Temperature Distribution in Submerged Arc Welding Process,'' *Advances in Materials Science and Engineering* ,Volume 2013, Article ID 543594, p.9, 2013.

[13] S. Alam, M.I. Khan, ''Predıctıon of weld bead penetratıon for steel usıng submerged arc weldıng process parameters,'' *International Journal of Engineering Science and Technology*, Vol. 3 No.10 2011.

[14] J. Nowacki, P. Rybicki, ''The influence of welding heat input on submerged arc welded duplex steel joints imperfections,'' *Journal of Materials Processing Technology*, Volumes 164–165, pp. 1082–1088, 2005.

[15] D. Akbari, S. Far, '' Effect of the welding heat input on residual stresses in butt-welds of dissimilar pipe joints,'' *International Journal of Pressure Vessels and Piping*, Volume 86, Issue 11, pp. 769–776, 2009.

[16] T. Melfi, ''New codes requirements for calculating heat input,'' *Welding Journal*, pp. 61-63, 2010.

[17] S. Kou, *Welding metallurgy*, John Willey, USA 2nd edition, 2003.

[18]G.K.Bause, J.R.Mihalisin,*Superalloys, supercomposites and and superceramics*, Eds. Tien , J.K. Caulfied, Academics Press, Inc., pp 99-148, 1989.

[19] H.M.Wang, J.H. Zhang, Y.J.Tang, Z.Q.Hu, '' Rapidly solidified MC carbide morphogoies of a laser-glaze single-crystal nickel-base superalloy,'' Material *Science and Engineering* A-*Structural Materials Properties Microstructure and Processing*, vol. 156, no1, pp 109-116, 1992.

[20] M. El-Bealy, B.G. Thomas, ''Prediction of dendrite arm spacing for low alloy steel casting processes,'' *Metallurgical and Materials Transactions B*, Volume 27b, 1996.

[21] W. Loser, S. Thiem, M. Jurish, ''Solidification modeling of the micro structures in near-shape casting of steels,'' *Materials Science Engineering A*, Volume 173, pp. 323-326, 1993.

[22] Z. Aydoğmuş, O. Aydoğmuş, ''A Comparison of Artificial Neural Network and Extended Kalman Filter Based Sensorless Speed Estimation,'' *Measurement*, Vol. 63, pp. 152-158, 2015.

[23] H. Towsyfyan, G. Davoudi, B.H. Dehkordy, A. Kariminasab, ''Comparing the Regression Analysis and Artificial Neural Network in Modeling the Submerged Arc Welding (SAW) Process,'' *Research Journal of Applied Sciences, Engineering and Technology*, Volume 5, Issue 9, pp. 2701-2706, 2013.